Asymptotic Analysis of the Natural System Modes of Coupled Bodies in the Large-Separation Low-Frequency Regime

George W. Hanson, *Member, IEEE*, and Carl E. Baum, *Fellow, IEEE*

***Abstract*—In this paper, we examine the natural system modes (characteristic frequencies and currents) of two coupled bodies in the limit of large separation. It is known that when objects are oriented such that they may interact electromagnetically, natural modes of the coupled system occur. These modes differ from, but may be related to, the natural modes of the isolated bodies. For example, the first antisymmetric and symmetric system frequencies of two identical bodies separated by some intermediate distance spiral around the dominant natural frequency of the isolated body as separation is varied. As separation further increases, these system resonances tend toward the origin in the complex frequency plane, rather than approaching the isolated body-dominant natural frequency. Here we treat an N-body scattering problem in the limit of large separation by replacing the bodies with equivalent dipole moments. The natural frequencies are obtained as singular points in the scattering solution. For the special case of two coupled objects, a simple equation for the natural system frequencies is obtained that shows that the real radian-system frequency approaches the origin as $1/r$, independent of the relative orientation and type of the two bodies. The damping coefficient approaches the origin approximately logarithmically as a function of the body orientation and type. Using this formulation, the natural system modes of two coupled wires are investigated for large separation between the wires and compared to an integral equation solution.**

***Index Terms*— Asymptotic analysis, coupled bodies, natural resonance.**

I. Introduction

The electromagnetic response of coupled bodies is of interest in many applications, including target detection and identification. In this paper, we consider the frequency (s-plane) behavior of the system resonances of coupled objects in the limit of large separation.

In an early paper relating to the singularity expansion method (SEM), it was observed that the SEM frequencies of an isolated thin-wire scatterer can be grouped in layers in the s-plane nearly parallel to the $j\omega$ axis [1], [20]. These resonances are further identified by their position within these layers. This observation naturally leads to the notation for the complex frequencies $s_{n,1}^{0}$, where n denotes the nth pole as measured from the $\mathrm{Re}\,(s)$ axis in the lth layer, measured from the $j\omega$ axis.

Shortly after the above observations were made concerning isolated wires, the natural system frequencies of coupled wires were studied. It was found that these system resonances exhibited some interesting characteristics as wire separation was varied [2]. To simplify the discussion, consider two identical wires for which the system resonances can be divided into symmetric $(s_{n,1}^{s})$ and antisymmetric $(s_{n,1}^{a})$ modes [3], [21]. As observed in [2] for two thin-wire scatterers, the low-order system resonances $(s_{1,1}^{a;s})$ tended to spiral around the dominant isolated body resonance $(s_{1,1}^{0})$ as spacing between the objects was varied over some intermediate distance. As separation was further increased, the system resonances moved off toward the origin in the complex frequency plane, and other system modes from another layer moved in to take their place, again spiraling around $s_{1,1}^{0}$. Subsequent to [2], other papers further considered coupled wire scatterers [4]–[5].

The fact that the system frequencies eventually tended toward the origin as spacing is increased beyond some intermediate distance rather than tending toward the isolated-body limit was discussed in [2], and explained from a time-domain perspective in [6]. It was observed that the SEM system modes are global quantities for the coupled body system and have no clear physical interpretation prior to times when global modes can be established. Hence, in a two-body system the time period after which the scattered field from each body has interacted with the other body is designated as late time. During late time, the two objects interact electromagnetically and global system modes are established. As spacing between the objects becomes large relative to the largest linear dimension of each body, the system resonances tend toward low frequencies since the time for a wave to travel between the two bodies becomes long. Eventually, the spacing tends toward infinity, and the system resonances tend toward the origin.

Since the resonances of a coupled system are rigorously obtained from a complicated (usually integral) system of equations, simple approximate formulas, which describe the system resonance behavior as a function of body separation, are of interest. For intermediate separations, perturbation formulas have been obtained which relate the natural system frequencies to the natural frequencies of the isolated bodies. Two related classes of perturbation solution have been obtained, both based

Manuscript received July 21, 1997; revised July 13, 1998. This work was supported by the Air Force Office of Scientific Research, Summer Research Program.

G. W. Hanson is with the Department of Electrical Engineering and Computer Science, University of Wisconsin-Milwaukee, Milwaukee, WI 53211 USA.

C. E. Baum is with the Air Force Research Laboratory, Kirtland AFB, NM 87117 USA.

Publisher Item Identifier S 0018-926X(99)02210-3.

upon the exact integral-operator description of the coupled system. The first method yields a quasi-analytic formula for the system frequencies of an object and a mirror object separated by some intermediate distance. The resulting formula involves a numerically computed coefficient, which only depends upon the isolated object's characteristics multiplied by an exponential term, which is a function of the separation between the objects [7], [22]. This method was extended to model the interaction between an object and a layered medium in [8]. The second method is more numerical in nature, yet represents a considerable simplification of the exact IE's and is applicable to a more general system of coupled bodies [9]. The formulation described in [9] was subsequently applied to a variety of coupled objects [6], [10], [11].

In this paper, we present a scattering formulation for N coupled objects valid in the limit of large separation between all objects. The system of scatterers are replaced by interacting dipole moments, which is a suitable approximation for large separations. A simpler formulation is provided for two objects coupled in a mirror symmetric configuration. Singularities of the scattering solution are identified as natural frequencies leading to the characteristic equation for natural frequencies of the coupled system. The example of two coupled wires is considered to demonstrate the accuracy of the asymptotic method, where the natural system frequencies from the asymptotic formulation are compared to those generated from a full-wave integral equation solution. Some results for the natural currents are provided to examine their behavior in the corresponding limit.

II. Preliminary Relations

Consider Maxwell's curl equations for free-space in the two-sided Laplace transform domain

$$\begin{aligned}\nabla \times \vec{E}(\vec{r},s) &= -s\vec{B}(\vec{r},s) - \vec{J}^m(\vec{r},s)\\ \nabla \times \vec{H}(\vec{r},s) &= s\vec{D}(\vec{r},s) + \vec{J}^e(\vec{r},s).\end{aligned} \tag{1}$$

The relationships between fields and currents are given in terms of four Green's dyadics as [12]

$$\begin{aligned}\vec{E}(\vec{r},s) &= -s\mu_0\langle \overleftrightarrow{G}_{e,e}(\vec{r}|\vec{r}',s); \vec{J}^e(\vec{r}',s)\rangle\\ &\quad + \langle \overleftrightarrow{G}_{e,m}(\vec{r}|\vec{r}',s); \vec{J}^m(\vec{r}',s)\rangle\\ \vec{H}(\vec{r},s) &= -s\epsilon_0\langle \overleftrightarrow{G}_{h,m}(\vec{r}|\vec{r}',s); \vec{J}^m(\vec{r}',s)\rangle\\ &\quad + \langle \overleftrightarrow{G}_{h,e}(\vec{r}|\vec{r}',s); \vec{J}^e(\vec{r}',s)\rangle\end{aligned} \tag{2}$$

where the bracket notation indicates a real inner product with integration over common spatial coordinates (typically, volume or surface integration). The Green's dyadics are

$$\begin{aligned}\overleftrightarrow{G}_{e,e}(\vec{r}|\vec{r}',s) &= PV[\overleftrightarrow{1} - \gamma^{-2}\nabla\nabla]G(\vec{r}|\vec{r}',s)\\ &\quad + \gamma^{-2}\overleftrightarrow{L}(\vec{r})\delta(\vec{r}-\vec{r}')\end{aligned} \tag{3}$$

$$\overleftrightarrow{G}_{e,m}(\vec{r}|\vec{r}',s) = -\nabla G(\vec{r}|\vec{r}',s) \times \overleftrightarrow{1} \tag{4}$$

$$\overleftrightarrow{G}_{h,e}(\vec{r}|\vec{r}',s) = -\overleftrightarrow{G}_{e,m}(\vec{r}|\vec{r}',s) \tag{5}$$

$$\overleftrightarrow{G}_{h,m}(\vec{r}|\vec{r}',s) = \overleftrightarrow{G}_{e,e}(\vec{r}|\vec{r}',s) \tag{6}$$

where $G(\vec{r}|\vec{r}',s) = (\gamma e^{-\xi}/4\pi\xi)$ is the free-space scaler Green's function with $\gamma = (s/c), \xi = \gamma R, c = (\epsilon_0\mu_0)^{-1/2}$, and $R = |\vec{r} - \vec{r}'|$. The first term in (3) can be written as

$$\begin{aligned}&[\overleftrightarrow{1} - \gamma^{-2}\nabla\nabla]G(\vec{r}|\vec{r}',s)\\ &\quad = \frac{\gamma e^{-\xi}}{4\pi}\{[-2\xi^{-3} - 2\xi^{-2}]\vec{1}_R\vec{1}_R + [\xi^{-3}+\xi^{-2}+\xi^{-1}]\\ &\qquad \cdot [\overleftrightarrow{1} - \vec{1}_R\vec{1}_R]\}\\ &\quad = -\frac{\gamma e^{-\xi}}{4\pi}\{[3\vec{1}_R\vec{1}_R - \overleftrightarrow{1}](\xi^{-3}+\xi^{-2}) + [\vec{1}_R\vec{1}_R - \overleftrightarrow{R}]\\ &\qquad \cdot \xi^{-1}\}\end{aligned} \tag{7}$$

where $\vec{1}_R = (\vec{r} - \vec{r}'/|\vec{r} - \vec{r}'|)$ and $\overleftrightarrow{1} = \vec{1}_x\vec{1}_x + \vec{1}_y\vec{1}_y + \vec{1}_z\vec{1}_z$ is the identity dyadic. For later convenience, define

$$\begin{aligned}\overleftrightarrow{F}_{e,e}(\vec{r}|\vec{r}',s) \equiv \frac{e^{-\gamma R}}{4\pi}\Bigg\{&[3\vec{1}_R\vec{1}_R - \overleftrightarrow{1}]\left(\frac{1}{\epsilon_0 R^3} + \frac{sZ_0}{R^2}\right)\\ &+ [\vec{1}_R\vec{1}_R - \overleftrightarrow{1}]\frac{s^2\mu_0}{R}\Bigg\}\end{aligned} \tag{8}$$

with $Z_0 = \sqrt{\mu_0/\epsilon_0}$, such that the $\overleftrightarrow{G}_{e,e}$ term can be expressed as

$$\begin{aligned}\overleftrightarrow{G}_{e,e}(\vec{r}|\vec{r}',s) = PV\frac{-1}{s^2\mu_0}\overleftrightarrow{F}_{e,e}(\vec{r}|\vec{r}',s) + \gamma^{-2}\overleftrightarrow{L}(\vec{r})\\ \delta(\vec{r}-\vec{r}').\end{aligned} \tag{9}$$

The magnetic Green's dyadic $\overleftrightarrow{G}_{e,m}$ can be expressed as

$$\begin{aligned}\overleftrightarrow{G}_{e,m}(\vec{r}|\vec{r}',s) &= -\nabla G(\vec{r}|\vec{r}',s) \times \overleftrightarrow{1}\\ &= \frac{e^{-\gamma R}}{4\pi}\left[\frac{1}{R^2} + \frac{s}{RC}\right]\vec{1}_R \times \overleftrightarrow{1}\end{aligned} \tag{10}$$

where upon defining for later convenience

$$F_{e,m}(\vec{r}|\vec{r}',s) \equiv \frac{e^{-\gamma R}}{4\pi}\left(\frac{s\mu_0}{R^2} + \frac{s^2\mu_0}{RC}\right) \tag{11}$$

the magnetic Green's dyadic can be written as

$$\overleftrightarrow{G}_{e,m}(\vec{r}|\vec{r}',s) = \frac{1}{s\mu_0}F_{e,m}(\vec{r}|\vec{r}',s)\vec{1}_R \times \overleftrightarrow{1}. \tag{12}$$

In (3), the PV notation indicates that the corresponding term should be integrated in the principal value sense [13], where

$$\overleftrightarrow{L}(\vec{r}) = \frac{1}{4\pi}\int_{S_\delta}\frac{\vec{1}_S(\vec{r}')\vec{1}_{R'}(\vec{r}|\vec{r}')}{|\vec{r}-\vec{r}'|^2}\,dS' \tag{13}$$

is the depolarizing dyadic integral evaluated over the surface S_δ of the exclusion volume V_δ excluded in the PV integration. In (13), $\vec{1}_{R'}(\vec{r}|\vec{r}') = -\vec{1}_R(\vec{r}|\vec{r}') = \vec{1}_R(\vec{r}'|\vec{r})$ and $\vec{1}_S(\vec{r})$ is the unit normal vector to S at $\vec{r}$. Note that the $\overleftrightarrow{G}_{\{\substack{e,e\\h,m}\}}$ terms are properly interpreted as distributions.

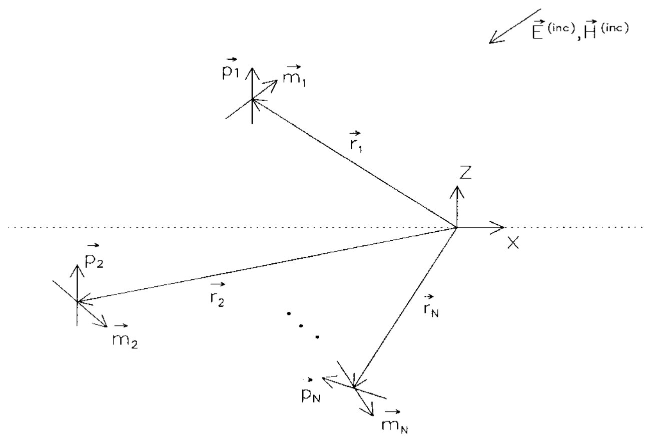

Fig. 1. Configuration of N interacting dipoles.

III. Scattering Formulation

Consider an N-body scattering problem, which can be analyzed by formulating a coupled set of integral equations for the current (surface or volume polarization) induced on/in the objects by an incident field. When the separation between all objects becomes large compared to the largest linear dimension of each object and in the limit of low frequency, the formulation can be considerably simplified by replacing each object with equivalent dipole moments. This follows from the fact that the electric and magnetic dipole moment terms dominant the fields due to a given current (as in a multipole expansion of the current) for large distances and low frequencies [14]. To formulate the desired set of equations, the scatterers, which are assumed to reside in free-space, are replaced with dipole moments $\overrightarrow{p}^{\beta}, \overrightarrow{m}^{\beta}$ for $\beta = 1, 2, \cdots, N$ corresponding to object $1, 2, \cdots N$, respectively, as shown in Fig. 1. The dipoles are considered to be generated by fields via polarizability dyadics as

$$\begin{aligned}\overrightarrow{p}^{(\beta)}(s) &= \epsilon_0 \overleftrightarrow{P}^{(\beta)}(s) \cdot \overrightarrow{E}(\overrightarrow{r}_\beta, s)\\ \overrightarrow{m}^{(\beta)}(s) &= \overleftrightarrow{M}^{(\beta)}(s) \cdot \overrightarrow{H}(\overrightarrow{r}_\beta, s)\end{aligned} \tag{14}$$

where the fields $(\overrightarrow{E}, \overrightarrow{H})$ are the total fields due to all dipoles not located at $\overrightarrow{r}_\beta$, plus any externally impressed field. The polarizability dyadics are symmetrical for reciprocal media

$$\begin{aligned}\overleftrightarrow{P}^{(\beta)^T}(s) &= \overleftrightarrow{P}^{(\beta)}(s)\\ \overleftrightarrow{M}^{(\beta)^T}(s) &= \overleftrightarrow{M}^{(\beta)}(s)\end{aligned} \tag{15}$$

and as $s \to 0$ [14]

$$\begin{aligned}\overleftrightarrow{P}^{(\beta)}(s) &= \overleftrightarrow{P}_0^{(\beta)} + O(s)\\ \overleftrightarrow{M}^{(\beta)}(s) &= \overleftrightarrow{M}_0^{(\beta)} + O(s).\end{aligned} \tag{16}$$

The currents associated with the dipole moments are

$$\begin{aligned}\overrightarrow{J}_e^{(\beta)} &= s\overrightarrow{p}^{(\beta)}\delta(\overrightarrow{r} - \overrightarrow{r}_\beta)\\ \overrightarrow{J}_m^{(\beta)} &= s\mu_0\overrightarrow{m}^{(\beta)}\delta(\overrightarrow{r} - \overrightarrow{r}_\beta).\end{aligned} \tag{17}$$

Inserting (17) into (2) leads to the fields at $\overrightarrow{r}_\alpha$ maintained by electric and magnetic dipoles located at $\overrightarrow{r}_\beta$ as

$$\begin{aligned}\overrightarrow{E}^{(\alpha,\beta)}(\overrightarrow{r}_\alpha, s) =& \overleftrightarrow{F}_{e,e}(\overrightarrow{r}_\alpha|\overrightarrow{r}_\beta, s) \cdot \overrightarrow{p}^{(\beta)}(s)\\ &+ F_{e,m}(\overrightarrow{r}_\alpha|\overrightarrow{r}_\beta, s)(\overrightarrow{1}_{R_{\alpha,\beta}} \times \overleftrightarrow{1})\\ &\cdot \overrightarrow{m}^{(\beta)}(s)\\ \overrightarrow{H}^{(\alpha,\beta)}(\overrightarrow{r}_\alpha, s) =& -\frac{1}{\mu_0}F_{e,m}(\overrightarrow{r}_\alpha|\overrightarrow{r}_\beta, s)(\overrightarrow{1}_{R_{\alpha,\beta}} \times \overleftrightarrow{1})\\ &\cdot \overrightarrow{p}^{(\beta)}(s) + \epsilon_0\overleftrightarrow{F}_{e,e}(\overrightarrow{r}_\alpha|\overrightarrow{r}_\beta, s)\\ &\cdot \overrightarrow{m}^{(\beta)}(s)\end{aligned} \tag{18}$$

where

$$\begin{aligned}\overleftrightarrow{F}_{e,e}(\overrightarrow{r}_\alpha|\overrightarrow{r}_\beta, s) =& \frac{e^{-\gamma R_{\alpha,\beta}}}{4\pi}\Bigg\{[3\overrightarrow{1}_{R_{\alpha,\beta}}\overrightarrow{1}_{R_{\alpha,\beta}} - \overleftrightarrow{1}]\\ &\left(\frac{1}{\epsilon_0 R_{\alpha,\beta}^3} + \frac{sZ_0}{R_{\alpha,\beta}^2}\right)\\ &+ [\overrightarrow{1}_{R_{\alpha,\beta}}\overrightarrow{1}_{R_{\alpha,\beta}} - \overleftrightarrow{1}]\frac{s^2\mu_0}{R_{\alpha,\beta}}\Bigg\}\\ F_{e,m}(\overrightarrow{r}_\alpha|\overrightarrow{r}_\beta, s) =& \frac{e^{-\gamma R_{\alpha,\beta}}}{4\pi}\left\{\frac{\mu_0 s}{R_{\alpha,\beta}^2} + \frac{\mu_0 s^2}{R_{\alpha,\beta}C}\right\}\end{aligned} \tag{19}$$

with $\overrightarrow{l}_{R_{\alpha,\beta}} = (\overrightarrow{r}_\alpha - \overrightarrow{r}_\beta)/|\overrightarrow{r}_\alpha - \overrightarrow{r}_\beta|$ being the unit vector from $\overrightarrow{r}_\beta$ to $\overrightarrow{r}_\alpha$ and $R_{\alpha,\beta} = |\overrightarrow{r}_\alpha - \overrightarrow{r}_\beta|$. The total field at $\overrightarrow{r}_\alpha$ due to $N-1$ dipoles located at $\overrightarrow{r}_\beta, \beta = 1, 2, \cdots, N, \beta \neq \alpha$ is

$$\begin{aligned}\overrightarrow{E}(\overrightarrow{r}_\alpha, s) &= \sum_{\substack{\beta=1\\ \beta\neq\alpha}}^{N} \overrightarrow{E}^{(\alpha,\beta)}(\overrightarrow{r}_\alpha, s)\\ \overrightarrow{H}(\overrightarrow{r}_\alpha, s) &= \sum_{\substack{\beta=1\\ \beta\neq\alpha}}^{N} \overrightarrow{H}^{(\alpha,\beta)}(\overrightarrow{r}_\alpha, s).\end{aligned} \tag{20}$$

Considering the scatterers to be as shown in Fig. 1, a coupled system of equations for the induced dipole moments can be written down as

$$\begin{aligned}\overrightarrow{p}^{(\alpha)}(s) &= \epsilon_0\overleftrightarrow{P}_0^{(\alpha)} \cdot \left[\overrightarrow{E}^{(\text{inc})}(\overrightarrow{r}_\alpha, s) + \sum_{\substack{\beta=1\\ \beta\neq\alpha}}^{N} \overrightarrow{E}^{(\alpha,\beta)}(\overrightarrow{r}_\alpha, s)\right]\\ \overrightarrow{m}^{(\alpha)}(s) &= \overleftrightarrow{M}_0^{(\alpha)} \cdot \left[\overrightarrow{H}^{(\text{inc})}(\overrightarrow{r}_\alpha, s) + \sum_{\substack{\beta=1\\ \beta\neq\alpha}}^{N} \overrightarrow{H}^{(\alpha,\beta)}(\overrightarrow{r}_\alpha, s)\right],\\ &\alpha = 1, 2, \cdots, N\end{aligned} \tag{21}$$

where the fields $(\overrightarrow{E}^{(\text{inc})}, \overrightarrow{H}^{(\text{inc})})$ are externally impressed fields. Defining

$$\begin{aligned}\overleftrightarrow{F}_{e,e}^{(\alpha,\beta)} &\equiv \overleftrightarrow{F}_{e,e}(\overrightarrow{r}_\alpha|\overrightarrow{r}_\beta, s)\\ F_{e,m}^{(\alpha,\beta)} &\equiv F_{e,m}(\overrightarrow{r}_\alpha|\overrightarrow{r}_\beta, s) = F_{e,m}(\overrightarrow{r}_\beta|\overrightarrow{r}_\alpha, s)\end{aligned} \tag{22}$$

the set of (21) can be written as

$$\begin{aligned}
&\vec{p}^{(\alpha)}(s) - \epsilon_0 \overleftrightarrow{P}_0^{(\alpha)} \cdot \sum_{\beta=1 \beta\neq\alpha}^{N} [\overleftrightarrow{F}_{e,e}^{(\alpha,\beta)} \cdot \vec{p}^{(\beta)} \\
&\qquad + F_{e,m}^{(\alpha,\beta)} (\vec{1}_{R_{\alpha,\beta}} \times \overleftrightarrow{1}) \cdot \vec{m}^{(\beta)}] \\
&\quad = \epsilon_0 \overleftrightarrow{P}_0^{(\alpha)} \cdot \vec{E}^{(\mathrm{inc})}(\vec{r}_\alpha, s) \\
&\vec{m}^{(\alpha)}(s) - \overleftrightarrow{M}_0^{(\alpha)} \cdot \sum_{\substack{\beta=1\\ \beta\neq\alpha}}^{N} \Bigg[-\frac{1}{\mu_0} F_{e,m}^{(\alpha,\beta)} (\vec{1}_{R_{\alpha,\beta}} \times \overleftrightarrow{1}) \\
&\qquad \cdot \vec{p}^{(\beta)} + \epsilon_0 \overleftrightarrow{F}_{e,e}^{(\alpha,\beta)} \cdot \vec{m}^{(\beta)} \Bigg] \\
&\quad = \overleftrightarrow{M}_0^{(\alpha)} \cdot \vec{H}^{(\mathrm{inc})}(\vec{r}_\alpha, s), \qquad \alpha = 1, 2, \cdots, N
\end{aligned} \tag{23}$$

It is convenient to write the above in block dyadic form

$$\begin{bmatrix}
\overleftrightarrow{1}_{2\times 2} & \overleftrightarrow{Q}_{2\times 2}^{(1,2)}(s) & \overleftrightarrow{Q}_{2\times 2}^{(1,3)}(s) & \cdots & \overleftrightarrow{Q}_{2\times 2}^{(1,N)}(s) \\
\overleftrightarrow{Q}_{2\times 2}^{(2,1)}(s) & \overleftrightarrow{l}_{2\times 2} & \overleftrightarrow{Q}_{2\times 2}^{(2,3)}(s) & \cdots & \overleftrightarrow{Q}_{2\times 2}^{(2,N)}(s) \\
\overleftrightarrow{Q}_{2\times 2}^{(3,1)}(s) & \overleftrightarrow{Q}_{2\times 2}^{(3,2)}(s) & \overleftrightarrow{1}_{2\times 2} & \cdots & \overleftrightarrow{Q}_{2\times 2}^{(3,N)}(s) \\
\vdots & \vdots & \vdots & \vdots & \vdots \\
\overleftrightarrow{Q}_{2\times 2}^{(N,1)}(s) & \overleftrightarrow{Q}_{2\times 2}^{(N,2)}(s) & \overleftrightarrow{Q}_{2\times 2}^{(N,3)}(s) & \cdots & \overleftrightarrow{l}_{2\times 2}
\end{bmatrix}
\cdot \begin{bmatrix} \vec{d}_{2\times 1}^{(1)}(s) \\ \vec{d}_{2\times 1}^{(2)}(s) \\ \vec{d}_{2\times 1}^{(3)}(s) \\ \vdots \\ \vec{d}_{2\times 1}^{(N)}(s) \end{bmatrix}
= \begin{bmatrix} \vec{F}_{2\times 1}^{(1)}(s) \\ \vec{F}_{2\times 1}^{(2)}(s) \\ \vec{F}_{2\times 1}^{(3)}(s) \\ \vdots \\ \vec{F}_{2\times 1}^{(N)}(s) \end{bmatrix} \tag{24}$$

where (25) (shown at the bottom of the page)

$$\begin{aligned}
\overleftrightarrow{1}_{2\times 2} &\equiv \begin{bmatrix} \overleftrightarrow{1} & \overleftrightarrow{0} \\ \overleftrightarrow{0} & \overleftrightarrow{1} \end{bmatrix}, \quad \vec{d}_{2\times 1}^{(\alpha)}(s) \equiv \begin{bmatrix} \vec{p}^{(\alpha)}(s) \\ \vec{m}^{(\alpha)}(s) \end{bmatrix} \\
\vec{F}_{2\times 1}^{(\alpha)}(s) &\equiv \begin{bmatrix} \epsilon_0 \overleftrightarrow{P}_0^{(\alpha)} \cdot \vec{E}^{(\mathrm{inc})}(\vec{r}_\alpha, s) \\ \overleftrightarrow{M}_0^{(\alpha)} \cdot \vec{H}^{(\mathrm{inc})}(\vec{r}_\alpha, s) \end{bmatrix}.
\end{aligned} \tag{26}$$

Providing that the left-hand dyadic matrix is nonsingular (24) can be inverted to yield (27), shown at the bottom of the page. Equation (27) provides a formal solution to the scattering problem for configurations and frequencies such that the dipole moment approximation is valid. Scattered fields are obtained by substituting (27) into (20).

Each dyadic block, with the exception of the identity blocks, is a function of complex frequency s. In this paper, we are primarily interested in determining the natural frequencies such that the left-hand block-dyadic matrix is singular. At a natural frequency

$$\det \begin{bmatrix}
\overleftrightarrow{1}_{2\times 2} & \overleftrightarrow{Q}_{2\times 2}^{(1,2)}(s) & \overleftrightarrow{Q}_{2\times 2}^{(1,3)}(s) & \cdots & \overleftrightarrow{Q}_{2\times 2}^{(1,N)}(s) \\
\overleftrightarrow{Q}_{2\times 2}^{(2,1)}(s) & \overleftrightarrow{1}_{2\times 2} & \overleftrightarrow{Q}_{2\times 2}^{(2,3)}(s) & \cdots & \overleftrightarrow{Q}_{2\times 2}^{(2,N)}(s) \\
\overleftrightarrow{Q}_{2\times 2}^{(3,1)}(s) & \overleftrightarrow{Q}_{2\times 2}^{(3,2)}(s) & \overleftrightarrow{1}_{2\times 2} & \cdots & \overleftrightarrow{Q}_{2\times 2}^{(3,N)}(s) \\
\vdots & \vdots & \vdots & \vdots & \vdots \\
\overleftrightarrow{Q}_{2\times 2}^{(N,1)}(s) & \overleftrightarrow{Q}_{2\times 2}^{(N,2)}(s) & \overleftrightarrow{Q}_{2\times 2}^{(N,3)}(s) & \cdots & \overleftrightarrow{1}_{2\times 2}
\end{bmatrix} = 0 \tag{28}$$

which forms the fundamental characteristic equation for natural system frequencies of N interacting objects in the large-separation low-frequency regime.

For the special case of two interacting dipoles

$$\begin{bmatrix} \vec{d}_{2\times 1}^{(1)}(s) \\ \vec{d}_{2\times 1}^{(2)}(s) \end{bmatrix} = \begin{bmatrix} \overleftrightarrow{1}_{2\times 2} & \overleftrightarrow{Q}_{2\times 2}^{(1,2)}(s) \\ \overleftrightarrow{Q}_{2\times 2}^{(2,1)}(s) & \overleftrightarrow{1}_{2\times 2} \end{bmatrix}^{-1} \cdot \begin{bmatrix} \vec{F}_{2\times 1}^{(1)}(s) \\ \vec{F}_{2\times 1}^{(2)}(s) \end{bmatrix} \tag{29}$$

where [15]

$$\begin{bmatrix} \overleftrightarrow{1}_{2\times 2} & \overleftrightarrow{Q}_{2\times 2}^{(1,2)} \\ \overleftrightarrow{Q}_{2\times 2}^{(2,1)} & \overleftrightarrow{1}_{2\times 2} \end{bmatrix}^{-1} = \begin{bmatrix} \overleftrightarrow{A}_{2\times 2} & \overleftrightarrow{B}_{2\times 2} \\ \overleftrightarrow{C}_{2\times 2} & \overleftrightarrow{D}_{2\times 2} \end{bmatrix} \tag{30}$$

with

$$\begin{aligned}
\overleftrightarrow{A}_{2\times 2} &= [\overleftrightarrow{1}_{2\times 2} - \overleftrightarrow{Q}_{2\times 2}^{(1,2)} \cdot \overleftrightarrow{1}_{2\times 2}^{-1} \cdot \overleftrightarrow{Q}_{2\times 2}^{(2,1)}]^{-1} \\
\overleftrightarrow{B}_{2\times 2} &= -[\overleftrightarrow{1}_{2\times 2} - \overleftrightarrow{Q}_{2\times 2}^{(1,2)} \cdot \overleftrightarrow{1}_{2\times 2}^{-1} \cdot \overleftrightarrow{Q}_{2\times 2}^{(2,1)}]^{-1} \cdot \overleftrightarrow{Q}_{2\times 2}^{(1,2)} \cdot \overleftrightarrow{1}_{2\times 2}^{-1} \\
&= -\overleftrightarrow{A}_{2\times 2} \cdot \overleftrightarrow{Q}_{2\times 2}^{(1,2)} \\
\overleftrightarrow{D}_{2\times 2} &= [\overleftrightarrow{1}_{2\times 2} - \overleftrightarrow{Q}_{2\times 2}^{(2,1)} \cdot \overleftrightarrow{1}_{2\times 2}^{-1} \cdot \overleftrightarrow{Q}_{2\times 2}^{(1,2)}]^{-1} \\
\overleftrightarrow{C}_{2\times 2} &= -[\overleftrightarrow{1}_{2\times 2} - \overleftrightarrow{Q}_{2\times 2}^{(2,1)} \cdot \overleftrightarrow{1}_{2\times 2}^{-1} \cdot \overleftrightarrow{Q}_{2\times 2}^{(1,2)}]^{-1} \cdot \overleftrightarrow{Q}_{2\times 2}^{(2,1)} \cdot \overleftrightarrow{1}_{2\times 2}^{-1} \\
&= -\overleftrightarrow{D}_{2\times 2} \cdot \overleftrightarrow{Q}_{2\times 2}^{(2,1)}.
\end{aligned} \tag{31}$$

$$\overleftrightarrow{Q}_{2\times 2}^{(\alpha,\beta)}(s) = \begin{bmatrix} -\epsilon_0 \overleftrightarrow{P}_0^{(\alpha)} \cdot \overleftrightarrow{F}_{e,e}^{(\alpha,\beta)} & -\epsilon_0 F_{e,m}^{(\alpha,\beta)} \overleftrightarrow{P}_0^{(\alpha)} \cdot (\vec{1}_{R_{\alpha,\beta}} \times \overleftrightarrow{1}) \\ \frac{1}{\mu_0} F_{e,m}^{(\alpha,\beta)} \overleftrightarrow{M}_0^{(\alpha)} \cdot (\vec{1}_{R_{\alpha,\beta}} \times \overleftrightarrow{1}) & -\epsilon_0 \overleftrightarrow{M}_0^{(\alpha)} \cdot \overleftrightarrow{F}_{e,e}^{(\alpha,\beta)} \end{bmatrix} \tag{25}$$

$$\begin{bmatrix} \vec{d}_{2\times 1}^{(1)}(s) \\ \vec{d}_{2\times 1}^{(2)}(s) \\ \vec{d}_{2\times 1}^{(3)}(s) \\ \vdots \\ \vec{d}_{2\times 1}^{(N)}(s) \end{bmatrix} = \begin{bmatrix}
\overleftrightarrow{1}_{2\times 2} & \overleftrightarrow{Q}_{2\times 2}^{(1,2)}(s) & \overleftrightarrow{Q}_{2\times 2}^{(1,3)}(s) & \cdots & \overleftrightarrow{Q}_{2\times 2}^{(1,N)}(s) \\
\overleftrightarrow{Q}_{2\times 2}^{(2,1)} & \overleftrightarrow{1}_{2\times 2} & \overleftrightarrow{Q}_{2\times 2}^{(2,3)}(s) & \cdots & \overleftrightarrow{Q}_{2\times 2}^{(2,N)}(s) \\
\overleftrightarrow{Q}_{2\times 2}^{(3,1)} & \overleftrightarrow{Q}_{2\times 2}^{(3,2)}(s) & \overleftrightarrow{1}_{2\times 2} & \cdots & \overleftrightarrow{Q}_{2\times 2}^{(3,N)}(s) \\
\vdots & \vdots & \vdots & \vdots & \vdots \\
\overleftrightarrow{Q}_{2\times 2}^{(N,1)}(s) & \overleftrightarrow{Q}_{2\times 2}^{(N,2)}(s) & \overleftrightarrow{Q}_{2\times 2}^{(N,3)}(s) & \cdots & \overleftrightarrow{1}_{2\times 2}
\end{bmatrix}^{-1} \cdot \begin{bmatrix} \vec{F}_{2\times 1}^{(1)}(s) \\ \vec{F}_{2\times 1}^{(2)}(s) \\ \vec{F}_{2\times 1}^{(3)}(s) \\ \vdots \\ \vec{F}_{2\times 1}^{(N)}(s) \end{bmatrix} \tag{27}$$

For two interacting dipoles, (28) becomes

$$\det\begin{bmatrix}\overleftrightarrow{1}_{2\times 2} & \overleftrightarrow{Q}^{(1,2)}_{2\times 2}\\ \overleftrightarrow{Q}^{(2,1)}_{2\times 2} & \overleftrightarrow{1}_{2\times 2}\end{bmatrix} = \det[\overleftrightarrow{1}_{2\times 2}]\det[\overleftrightarrow{1}_{2\times 2} - \overleftrightarrow{Q}^{(2,1)}_{2\times 2}\cdot\overleftrightarrow{1}^{-1}_{2\times 2}\cdot\overleftrightarrow{Q}^{(1,2)}_{2\times 2}] = \det[\overleftrightarrow{1}_{2\times 2} - \overleftrightarrow{Q}^{(2,1)}_{2\times 2}\cdot\overleftrightarrow{Q}^{(1,2)}_{2\times 2}] = 0. \tag{32}$$

IV. Characteristic Equation for Thin Wires

At this point, it is instructive to examine a special case of (32). Consider two nonidentical objects with $\overleftrightarrow{M}^{(1)} = \overleftrightarrow{M}^{(2)} = \overleftrightarrow{0}$. In this case, the two nontrivial block-dyadics are

$$\overleftrightarrow{Q}^{(\alpha,\beta)}_{2\times 2} = \begin{bmatrix}-\epsilon_0\overleftrightarrow{P}^{(\alpha)}_0\cdot\overleftrightarrow{F}^{(\alpha,\beta)}_{e,e} & \overleftrightarrow{0}\\ \overleftrightarrow{0} & \overleftrightarrow{0}\end{bmatrix} \tag{33}$$

leading to

$$\det[\overleftrightarrow{1} - \epsilon_0^2\overleftrightarrow{P}^{(2)}_0\cdot\overleftrightarrow{F}^{(2,1)}_0\cdot\overleftrightarrow{P}^{(1)}_0\cdot\overleftrightarrow{F}^{(1,2)}_{e,e}] = 0. \tag{34}$$

As an example, consider thin perfectly conducting wires oriented along the α direction for which $\overleftrightarrow{P}_0 = P_0\overleftrightarrow{1}_\alpha\overleftrightarrow{1}_\alpha$ and the magnetic polarizability dyadic is negligible. A prolate spheroid model of a wire with semi-major axis $L/2$ and semi-minor axis a results in [16]

$$P_0 = \frac{4}{3}\pi\left(\frac{L}{2}\right)^2\left[1-\left(\frac{2a}{L}\right)\right]\left\{\frac{1}{2}\left[1-\left(\frac{2a}{L}\right)^2\right]^{-1/2} \ln\left[\frac{1+\left[1-\left(\frac{2a}{L}\right)^2\right]^{1/2}}{1-\left[1-\left(\frac{2a}{L}\right)^2\right]^{1/2}}\right] - 1\right\}^{-1} = \frac{4}{3}\pi\left(\frac{L}{2}\right)^3\left[\ln\left(\frac{L}{a}\right)-1\right]^{-1} \quad \text{as } \frac{a}{L}\to 0. \tag{35}$$

Now, consider three different orientations of the wires. For simplicity, in each case, the wires will be located at $\vec{r}_{\frac{1}{2}} = x_0\vec{1}_x + y_0\vec{1}_y \pm (r/2)\vec{1}_z$ such that $\overleftrightarrow{F}^{(2,1)}_{e,e} = \overleftrightarrow{F}^{(1,2)}_{e,e}$.

Case A—Parallel Wires: Consider the wires to be oriented parallel to the x axis of Fig. 1 such that $\overleftrightarrow{P}^{(\alpha)}_0 = \vec{r}_x\vec{1}_x P^{(\alpha)}_0$ with $P^{(\alpha)}_0$ defined by (35). The governing (34) becomes

$$\det[\overleftrightarrow{1} - \epsilon_0^2\overleftrightarrow{P}^{(2)}_0\cdot\overleftrightarrow{F}^{(2,1)}_{e,e}\cdot\overleftrightarrow{P}^{(1)}_0\cdot\overleftrightarrow{F}^{(1,2)}_{e,e}] = 1 - \epsilon_0^2 P^{(2)}_0 P^{(1)}_0\left[\left(\frac{e^{-\gamma r}}{4\pi}\right)\left(\frac{1}{r^3\epsilon_0} + \frac{Z_0 s}{r^2} + \frac{\mu_0 s}{r}\right)\right]^2 = 0. \tag{36}$$

Making the substitution $\Gamma = \gamma r$ yields

$$e^{-\Gamma}(1+\Gamma+\Gamma^2) = \pm\frac{r^2 4\pi}{\sqrt{P^{(2)}_0 P^{(1)}_0}} \tag{37}$$

which is the characteristic equation for the natural system frequencies of two nonidentical parallel wires in the large-separation limit. The solution of (37) for the special case of two identical wires will be considered in Section VII. If we further assume the same length-to-radius ratio for both wires $L^{(1)}/a^{(1)} = L^{(2)}/a^{(2)} = L_a$, then $P^{(1,2)}_0 = K[L^{(1,2)}]^3$ with $K = (\pi/6)[\ln(L_a)^{-1}]^{-1}$ (37) can be written more directly in terms of the three parameters $r, L^{(1)}, L^{(2)}$ as

$$e^{-\Gamma}(1+\Gamma+\Gamma^2) = \pm\left(\frac{r}{L^{(2)}}\right)^{3/2}\left(\frac{r}{L^{(1)}}\right)^{3/2}\frac{4\pi}{k}. \tag{38}$$

Case B—Colinear Wires: Consider two colinear wires aligned parallel to the z axis of Fig. 1 such that $\overleftrightarrow{P}^{(\alpha)}_0 = \vec{1}_z\vec{1}_z P^{(\alpha)}_0$ with $P^{(\alpha)}_0$ defined by (35). The governing characteristic (34) becomes

$$\det[\overleftrightarrow{1} - \epsilon_0^2\overleftrightarrow{P}^{(2)}_0\cdot\overleftrightarrow{F}^{(2,1)}_{e,e}\cdot\overleftrightarrow{P}^{(1)}_0\cdot\overleftrightarrow{F}^{(1,2)}_{e,e}] = 1 - \epsilon_0^2 P^{(2)}_0 P^{(1)}_0\left[\left(\frac{e^{-\gamma r}}{2\pi}\right)\left(\frac{1}{r^3\epsilon_0} + \frac{Z_0 s}{r^2}\right)\right]^2 = 0 \tag{39}$$

resulting in

$$e^{-\Gamma}(1+\Gamma) = \pm\frac{r^3 2\pi}{\sqrt{P^{(2)}_0 P^{(1)}_0}} \tag{40}$$

which is the characteristic equation for the natural system frequencies of two nonidentical colinear wires in the large-separation limit. For $L^{(1)}/a^{(1)} = L^{(2)}/a^{(2)} = L_a$ such that $P^{(1,2)}_0 = K[L^{(1,2)}]^3$ with k as defined previously, (40) can be written as

$$e^{-\Gamma}(1+\Gamma) = \pm\left(\frac{r}{L^{(2)}}\right)^{3/2}\left(\frac{r}{L^{(1)}}\right)^{3/2}\frac{2\pi}{k}. \tag{41}$$

Case C—Perpendicularly Oriented Wires: To analyze two wires oriented perpendicularly to each other, one may take, for instance, $\overleftrightarrow{P}^{(1)}_0 = \vec{1}_x\vec{1}_x P^{(1)}_0$ and $\overleftrightarrow{P}^{(2)}_0 = \vec{1}_z\vec{1}_z P^{(2)}_0$. The characteristic (34) becomes

$$\det[\overleftrightarrow{l} - \epsilon_0^2\overleftrightarrow{P}^{(2)}_0\cdot\overleftrightarrow{F}^{(2,1)}_{e,e}\cdot\overleftrightarrow{P}^{(1)}_0\cdot\overleftrightarrow{F}^{(1,2)}_{e,e}] = \det[\overleftrightarrow{1} - \overleftrightarrow{0}] = 1 \tag{42}$$

so that no frequency exists to yield a singular matrix.

V. Scattering from a Dipole in the Presence of a Mirror Object

In this section, we will specialize the preceding formulation to the case of two interacting dipoles, which are mirror images of each other, as shown in Fig. 2. For simplicity, each dipole is located at $x = y = 0$ so that dipole one is located at $\vec{r}_1 = \vec{1}_z r/2$ and dipole two is located at $\vec{r}_2 = -\vec{1}_z r/2 = \overleftrightarrow{R}_z\cdot\vec{r}_1$ such that $\vec{1}_{R_{1,2}} = \vec{1}_z = -\vec{1}_{R_{2,1}}$, where [3], [21]

$$\overleftrightarrow{R}_z \equiv \begin{bmatrix}1 & 0 & 0\\ 0 & 1 & 0\\ 0 & 0 & -1\end{bmatrix} = \overleftrightarrow{R}^{-1}_z. \tag{43}$$

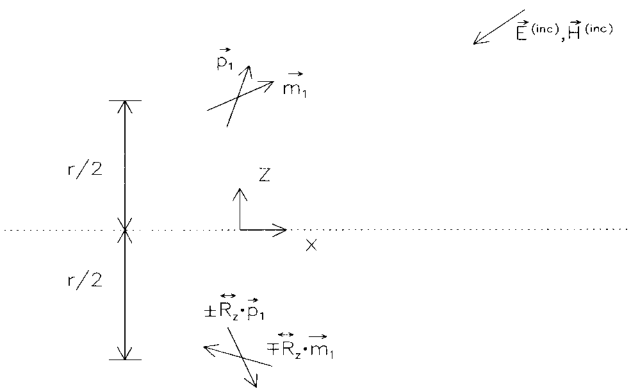

Fig. 2. Two mirror-symmetric dipoles, upper sign depicted.

The incident fields can be decomposed into symmetric and antisymmetric parts as [16]

$$\begin{aligned}\vec{E}^{(\mathrm{inc})}(\vec{r}_1,s)&=\tfrac{1}{2}\,[\vec{E}^{(\mathrm{inc})}(\vec{r}_1,s)\pm\overleftrightarrow{R}_z\cdot\vec{E}^{(\mathrm{inc})}(\vec{r}_2,s)]\\ \vec{E}^{(\mathrm{inc})}(\vec{r}_2,s)&=\tfrac{1}{2}\,[\vec{E}^{(\mathrm{inc})}(\vec{r}_2,s)\pm\overleftrightarrow{R}_z\cdot\vec{E}^{(\mathrm{inc})}(\vec{r}_1,s)]\\ \vec{H}^{(\mathrm{inc})}(\vec{r}_1,s)&=\tfrac{1}{2}\,[\vec{H}^{(\mathrm{inc})}(\vec{r}_1,s)\mp\overleftrightarrow{R}_z\cdot\vec{H}^{(\mathrm{inc})}(\vec{r}_2,s)]\\ \vec{H}^{(\mathrm{inc})}(\vec{r}_2,s)&=\tfrac{1}{2}\,[\vec{H}^{(\mathrm{inc})}(\vec{r}_2,s)\mp\overleftrightarrow{R}_z\cdot\vec{H}^{(\mathrm{inc})}(\vec{r}_1,s)].\end{aligned}\tag{44}$$

From the equation above, it is easily seen that

$$\begin{aligned}\vec{E}^{(\mathrm{inc})}(\vec{r}_1,s)&=\pm\overleftrightarrow{R}_z\cdot\vec{E}^{(\mathrm{inc})}(\vec{r}_2,s)\\ \vec{E}^{(\mathrm{inc})}(\vec{r}_2,s)&=\pm\overleftrightarrow{R}_z\cdot\vec{E}^{(\mathrm{inc})}(\vec{r}_1,s)\\ \vec{H}^{(\mathrm{inc})}(\vec{r}_1,s)&=\mp\overleftrightarrow{R}_z\cdot\vec{H}^{(\mathrm{inc})}(\vec{r}_2,s)\\ \vec{H}^{(\mathrm{inc})}(\vec{r}_2,s)&=\mp\overleftrightarrow{R}_z\cdot\vec{H}^{(\mathrm{inc})}(\vec{r}_1,s).\end{aligned}\tag{45}$$

With the relations

$$\begin{aligned}\overleftrightarrow{F}_{e,e}&\equiv\overleftrightarrow{F}_{e,e}(\vec{r}_\alpha|\vec{r}_\beta,s)=\overleftrightarrow{R}_z\cdot\overleftrightarrow{F}_{e,e}(\vec{r}_\beta|\vec{r}_\alpha,s)\cdot\overleftrightarrow{R}_z\\ \overleftrightarrow{P}_0^{(\alpha)}&=\overleftrightarrow{R}_z\cdot\overleftrightarrow{P}_0^{(\beta)}\cdot\overleftrightarrow{R}_z\\ \overleftrightarrow{M}_0^{(\alpha)}&=\overleftrightarrow{R}_z\cdot\overleftrightarrow{M}_0^{(\beta)}\cdot\overleftrightarrow{R}_z\\ \vec{p}^{(\alpha)}&=\pm\overleftrightarrow{R}_z\cdot\vec{p}^{(\beta)}=\pm\vec{p}^{(\beta)}\cdot\overleftrightarrow{R}_z\\ \vec{m}^{(\alpha)}&=\mp\overleftrightarrow{R}_z\cdot\vec{m}^{(\beta)}=\mp\vec{m}^{(\beta)}\cdot\overleftrightarrow{R}_z,\qquad\alpha\neq\beta\end{aligned}\tag{46}$$

the scattered fields are related by

$$\begin{aligned}\vec{E}^{(\alpha,\beta)}(\vec{r}_\alpha,s)&=\pm\overleftrightarrow{R}_z\cdot\vec{E}^{(\beta,\alpha)}(\vec{r}_\beta,s)\\ \vec{H}^{(\alpha,\beta)}(\vec{r}_\alpha,s)&=\mp\overleftrightarrow{R}_z\cdot\vec{H}^{(\beta,\alpha)}(\vec{r}_\beta,s).\end{aligned}\tag{47}$$

With (45)–(47), (23) becomes

$$\begin{aligned}&\vec{p}^{(1)}(s)\mp\epsilon_0\overleftrightarrow{P}_0^{(1)}\cdot[\overleftrightarrow{F}_{e,e}\cdot\overleftrightarrow{R}_z\cdot\vec{p}^{(1)}-F_{e,m}(\vec{1}_z\times\overleftrightarrow{R}_z)\\ &\quad\cdot\vec{m}^{(1)}]=\epsilon_0\overleftrightarrow{P}_0^{(1)}\cdot\vec{E}^{(\mathrm{inc})}(\vec{r}_1,s)\\ &\vec{m}^{(1)}(s)\pm\overleftrightarrow{M}_0^{(1)}\cdot\left[\frac{1}{\mu_0}F_{e,m}(\vec{1}_z\times\overleftrightarrow{R}_z)\cdot\vec{p}^{(1)}+\epsilon_0\overleftrightarrow{F}_{e,e}\right.\\ &\qquad\left.\cdot\overleftrightarrow{R}_z\cdot\vec{m}^{(1)}\right]=\overleftrightarrow{M}_0^{(1)}\cdot\overleftrightarrow{H}^{(\mathrm{inc})}(\vec{r}_1,s)\end{aligned}\tag{48}$$

which can be written in matrix form as

$$\begin{aligned}&\begin{bmatrix}\overleftrightarrow{1}\mp\epsilon_0\overleftrightarrow{P}_0^{(1)}\cdot\overleftrightarrow{F}_{e,e}\cdot\overleftrightarrow{R}_z & \pm\epsilon_0F_{e,m}\overleftrightarrow{P}_0^{(1)}\cdot(\vec{1}\times\overleftrightarrow{R}_z)\\ \pm\dfrac{1}{\mu_0}F_{e,m}\overleftrightarrow{M}_0^{(1)}\cdot(\vec{1}_z\times\overleftrightarrow{R}_z) & \overleftrightarrow{1}\pm\epsilon_0\overleftrightarrow{M}_0^{(1)}\cdot\overleftrightarrow{F}_{e,e}\cdot\overleftrightarrow{R}_z\end{bmatrix}\\ &\qquad\cdot\begin{bmatrix}\overleftrightarrow{p}^{(1)}(s)\\ \overleftrightarrow{m}^{(1)}(s)\end{bmatrix}=\begin{bmatrix}\epsilon_0\overleftrightarrow{P}_0^{(1)}\cdot\overleftrightarrow{E}^{(\mathrm{inc})}\\ \overleftrightarrow{M}_0^{(1)}\cdot\overleftrightarrow{H}^{(\mathrm{inc})}(s)\end{bmatrix}.\end{aligned}\tag{49}$$

Equation (49) is naturally decomposed into block dyadic form as

$$\begin{bmatrix}\overleftrightarrow{Q}_{pp}(s) & \overleftrightarrow{Q}_{pm}(s)\\ \overleftrightarrow{Q}_{mp}(s) & \overleftrightarrow{Q}_{mm}(s)\end{bmatrix}\cdot\begin{bmatrix}\overleftrightarrow{p}^{(1)}(s)\\ \overleftrightarrow{m}^{(1)}(s)\end{bmatrix}=\begin{bmatrix}\epsilon_0\overleftrightarrow{P}_0^{(1)}\cdot\overleftrightarrow{E}^{(\mathrm{inc})}(s)\\ \overleftrightarrow{M}_0^{(1)}\cdot\vec{H}^{(\mathrm{inc})}(s)\end{bmatrix}\tag{50}$$

where

$$\begin{aligned}\overleftrightarrow{Q}_{pp}(s)&\equiv\overleftrightarrow{1}\mp\epsilon_0\overleftrightarrow{P}_0^{(1)}\cdot\overleftrightarrow{F}_{e,e}\cdot\overleftrightarrow{R}_z\\ \overleftrightarrow{Q}_{pm}(s)&\equiv\pm\epsilon_0F_{e,m}\overleftrightarrow{P}_0^{(1)}\cdot(\vec{1}\times\overleftrightarrow{R}_z)\\ \overleftrightarrow{Q}_{mp}(s)&\equiv\pm\frac{1}{\mu_0}F_{e,m}\overleftrightarrow{M}_0^{(1)}\cdot(\vec{1}_z\times\overleftrightarrow{R}_z)\\ \overleftrightarrow{Q}_{mm}(s)&\equiv\overleftrightarrow{1}\pm\epsilon_0\overleftrightarrow{M}_0^{(1)}\cdot\overleftrightarrow{F}_{e,e}\cdot\overleftrightarrow{R}_z\end{aligned}\tag{51}$$

such that each block is a single dyadic expression rather than a matrix of dyadics as in (24). Providing that the left-hand dyadic matrix is nonsingular, (50) can be inverted in the same manner as (29) to yield

$$\begin{aligned}\begin{bmatrix}\vec{p}^{(1)}(s)\\ \vec{m}^{(1)}(s)\end{bmatrix}&=\begin{bmatrix}\overleftrightarrow{Q}_{pp}(s) & \overleftrightarrow{Q}_{pm}(s)\\ \overleftrightarrow{Q}_{mp}(s) & \vec{Q}_{mm}(s)\end{bmatrix}^{-1}\\ &\quad\cdot\begin{bmatrix}\epsilon\overleftrightarrow{P}_0^{(1)}\cdot\vec{E}^{(\mathrm{inc})}(s)\\ \overleftrightarrow{M}_0^{(1)}\cdot\vec{H}^{(\mathrm{inc})}(s)\end{bmatrix}\end{aligned}\tag{52}$$

where

$$\begin{bmatrix}\overleftrightarrow{Q}_{pp} & \overleftrightarrow{Q}_{pm}\\ \overleftrightarrow{Q}_{mp} & \overleftrightarrow{Q}_{mm}\end{bmatrix}^{-1}=\begin{bmatrix}\overleftrightarrow{A} & \overleftrightarrow{B}\\ \overleftrightarrow{C} & \overleftrightarrow{D}\end{bmatrix}\tag{53}$$

with

$$\begin{aligned}\overleftrightarrow{A}&=[\overleftrightarrow{Q}_{pp}-\overleftrightarrow{Q}_{pm}\cdot\overleftrightarrow{Q}_{mm}^{-1}\cdot\overleftrightarrow{Q}_{mp}]^{-1}\\ \overleftrightarrow{B}&=-[\overleftrightarrow{Q}_{pp}-\overleftrightarrow{Q}_{pm}\cdot\overleftrightarrow{Q}_{mm}^{-1}\cdot\overleftrightarrow{Q}_{mp}]^{-1}\cdot\vec{Q}_{pm}\cdot\overleftrightarrow{Q}_{mm}^{-1}\\ &=-\overleftrightarrow{A}\cdot\overleftrightarrow{Q}_{pm}\cdot\overleftrightarrow{Q}_{mm}^{-1}\\ \overleftrightarrow{D}&=[\overleftrightarrow{Q}_{mm}-\overleftrightarrow{Q}_{mp}\cdot\overleftrightarrow{Q}_{pp}^{-1}\cdot\overleftrightarrow{Q}_{pm}]^{-1}\\ \overleftrightarrow{C}&=-[\vec{Q}_{mm}-\overleftrightarrow{Q}_{mp}\cdot\overleftrightarrow{Q}_{pp}^{-1}\cdot\overleftrightarrow{Q}_{pm}]^{-1}\cdot\overleftrightarrow{Q}_{mp}\cdot\overleftrightarrow{Q}_{pp}^{-1}\\ &=-\overleftrightarrow{D}\cdot\overleftrightarrow{Q}_{mp}\cdot\overleftrightarrow{Q}_{pp}^{-1}.\end{aligned}\tag{54}$$

Equation (52) provides a formal solution to the mirror-symmetric scattering problem for configurations and frequencies such that the dipole moment approximation is valid. As in Section III, we are primarily interested in determining the natural frequencies such that the left-hand dyadic matrix is singular, leading to

$$\begin{aligned}&\det\begin{bmatrix}\overleftrightarrow{Q}_{pp} & \overleftrightarrow{Q}_{pm}\\ \overleftrightarrow{Q}_{mp} & \overleftrightarrow{Q}_{mm}\end{bmatrix}\\ &\quad=\det[\overleftrightarrow{Q}_{pp}]\det[\overleftrightarrow{Q}_{mm}-\overleftrightarrow{Q}_{mp}\cdot\overleftrightarrow{Q}_{pp}^{-1}\cdot\overleftrightarrow{Q}_{pm}]=0\end{aligned}\tag{55}$$

which forms the fundamental characteristic equation for natural system frequencies of two interacting mirror-symmetric objects in the large-separation low-frequency regime. In the following section, mirror-symmetric configurations of wires and loops will be considered. It should be noted in all of the results to follow, the upper and lower signs correspond to the symmetric and anti-symmetric modes, respectively.

VI. Characteristic Equation for Mirror-Symmetric Wires and Loops

Consider a thin perfectly conducting wire with $\overleftrightarrow{M}^{(1)} = \overleftrightarrow{0}$. Equation (55) reduces to

$$\det[\overleftrightarrow{Q}_{pp}] = \det[\overleftrightarrow{1} \mp \epsilon_0 \overleftrightarrow{P}_0^{(1)} \cdot \overleftrightarrow{F}_{e,e} \cdot \overleftrightarrow{R}_z] = 0 \qquad (56)$$

which can be written in matrix form as (57), shown at the bottom of the page, where

$$a_1 + \frac{1}{r^3\epsilon_0} + \frac{Z_0 s}{r^2}, \quad b = \frac{\mu_0 s^2}{r}. \qquad (58)$$

Now consider three different wire orientations.

Case A—Parallel Wires: Consider two parallel wires oriented along the x axis of Fig. 2 such that $\overleftrightarrow{P}_0^{(1)} = \vec{1}_x \vec{1}_x P_0$ with P_0 defined by (35). Equation (57) then becomes

$$1 \pm \epsilon_0 \frac{e^{-\gamma r}}{4\pi} P_0 \left(\frac{1}{r^3\epsilon_0} + \frac{Z_0 s^2}{r^2} + \frac{\mu_0 s^2}{r} \right) = 0. \qquad (59)$$

With $\Gamma = \gamma r$ as defined before, we get

$$e^{-\Gamma}(1 + \Gamma + \Gamma^2) = \mp \frac{r^3 4\pi}{P_0} \qquad (60)$$

which is the characteristic equation for the natural system frequencies of two identical parallel wires in the large-separation limit. Although this is merely a special case of (37) with $P_0^{(2)} = P_0^{(1)} = P_0$, it should be noted that the mirror-symmetric formulation leading to (60) is simpler than the general scattering formulation, justifying the usefulness of the separate derivation outlined in this section. The solution of (37) for the special case of two identical wires, i.e., (60), will be considered in Section VII.

Case B—Colinear Wires: Consider two colinear wires aligned along the z axis of Fig. 2, such that $\overleftrightarrow{P}_0^{(1)} = \vec{1}_z \vec{1}_z P_0$ with P_0 defined by (35). The governing characteristic equation (57) reduces to

$$1 \pm \epsilon_0 \frac{e^{-\gamma r}}{4\pi} 2P_0 \left(\frac{1}{r^3\epsilon_0} + \frac{Z_0 s^2}{r^2} \right) = 0 \qquad (61)$$

which can be written as

$$e^{-\Gamma}(1 + \Gamma) = \mp \frac{r^3 2\pi}{P_0} \qquad (62)$$

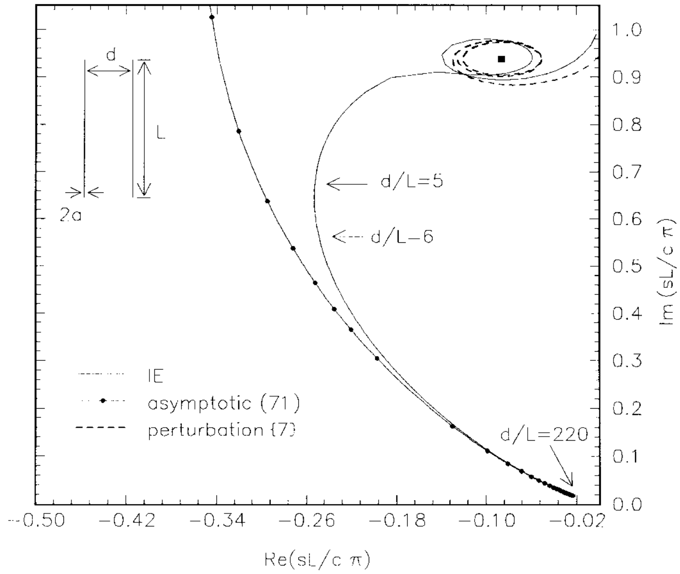

Fig. 3. Trajectory of lowest order antisymmetric mode of two identical parallel wires parameterized by separation distance, which varies from $d/L = 220$ to $d/L = 0.01$. Solid box is the location of the isolated-wire dominant natural resonance.

which is the characteristic equation for the natural system frequencies of two identical colinear wires in the large-separation limit. Note that (62) is merely a special case of (40) with $P_0^{(2)} = P_0^{(1)} = P_0$ although derived under the simpler mirror-symmetric formulation.

Case C—Mirror-Symmetric Wires Arbitrary Oriented in the x-z Plane: Consider one of the wires to lie in the x-z plane in Fig. 2 at an angle θ measured from the z axis, with the other wire in mirror-symmetric fashion. The polarizability dyadic for this case is

$$\begin{aligned}\overleftrightarrow{P}_0^{(1)} &= \vec{1}_{z'} \vec{1}_{z'} P_0 \\ &= [\vec{1}_z \vec{1}_z \cos^2(\theta) + \vec{1}_z \vec{1}_x \cos(\theta)\sin(\theta) + \vec{1}_x \vec{1}_z \\ &\quad \cos(\theta)\sin(\theta) + \vec{1}_x \vec{1}_z \sin^2(\theta)] P_0 \\ &= \vec{1}_z \vec{1}_z P_{zz} + \vec{1}_z \vec{1}_x P_{zx} + \vec{1}_x \vec{1}_z P_{xz} + \vec{1}_x \vec{1}_x P_{xx}\end{aligned} \qquad (63)$$

with P_0 defined by (35). The relevant characteristic equation (57) then becomes

$$\det \begin{bmatrix} 1 \pm \epsilon_0 \frac{e^{-\gamma r}}{4\pi} P_{xx}(a_1 + b_1) & 0 & \pm\epsilon_0 \frac{e^{-\gamma r}}{4\pi} P_{xz} 2a_1 \\ 0 & 1 & 0 \\ \pm\epsilon_0 \frac{e^{-\gamma r}}{4\pi} P_{zx}(a_1 + b_1) & 0 & 1 \pm \epsilon_0 \frac{e^{-\gamma r}}{4\pi} P_{zz} 2a_1 \end{bmatrix} = 0 \qquad (64)$$

$$\det \begin{bmatrix} 1 \pm \epsilon_0 \frac{e^{-\gamma r}}{4\pi} P_{xx}(a_1 + b_1) & \pm\epsilon_0 P_{xy}(a_1 + b_1) & \pm\epsilon_0 P_{xx} 2a_1 \\ \pm\epsilon_0 P_{yx}(a_1 + b_1) & 1 \pm \epsilon_0 \frac{e^{-\gamma r}}{4\pi} P_{yy}(a_1 + b_1) & \pm\epsilon_0 P_{yz} 2a_1 \\ \pm\epsilon_0 P_{zx}(a_1 + b_1) & \pm\epsilon_0 P_{zy}(a_1 + b_1) & 1 \pm \epsilon \frac{e^{-\gamma r}}{4\pi} P_{zz} 2a_1 \end{bmatrix} = 0 \qquad (57)$$

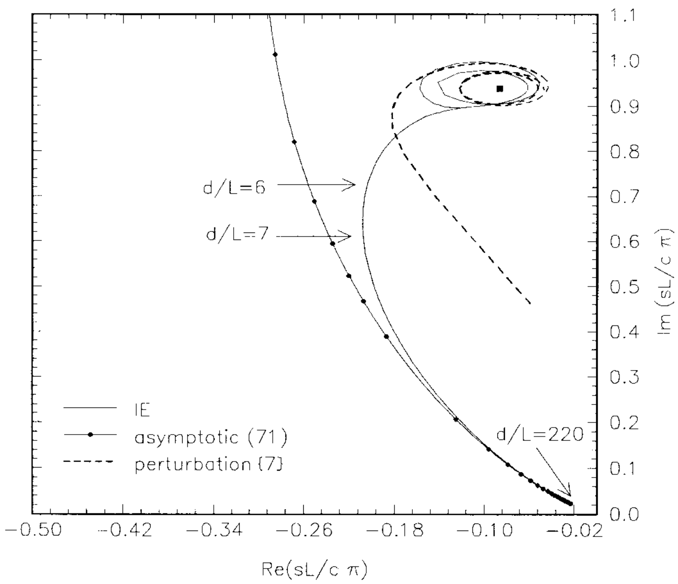

Fig. 4. Trajectory of lowest order symmetric mode of two identical parallel wires parameterized by separation distance, which varies from $d/L = 220$ to $d/L = 0.01$. Solid box is the location of the isolated wire-dominant natural resonance.

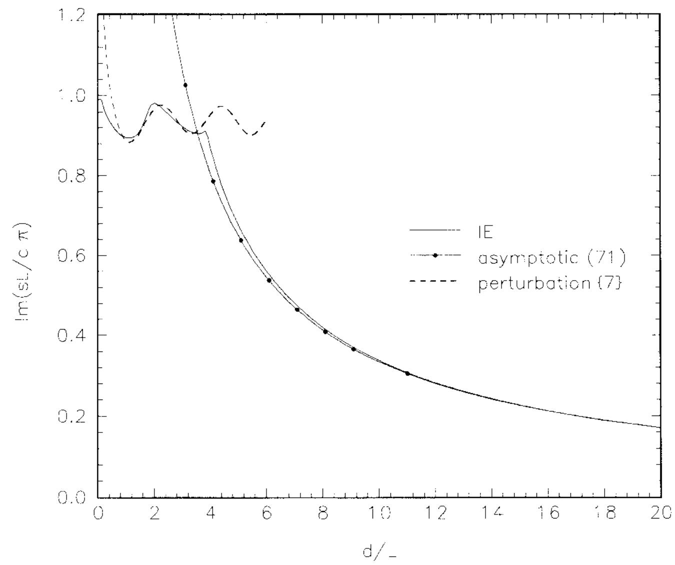

Fig. 5. Radian frequency of lowest order antisymmetric mode of two identical parallel wires versus separation distance.

leading to

$$e^{-\Gamma}\{\sin^2(\theta)(1+\Gamma+\Gamma^2)+\cos^2(\theta)+2(1+\Gamma)\} = \mp\frac{r^3 4\pi}{P_0}. \tag{65}$$

Note that (65) reduces to (62) for $\theta = 0$ and to (60) for $\theta = \pi/2$, as expected.

As another example, consider two parallel thin-wire loops with axes aligned along the z axis of Fig. 2 separated by a distance r, each having loop radius b and wire radius a. The polarizability dyadics are

$$\begin{aligned}\overleftrightarrow{p}^{(1)} &= \vec{1}_x\vec{1}_x P_{xx} + \vec{1}_y\vec{1}_y P_{yy}\\ \overleftrightarrow{M}^{(1)} &= \vec{1}_z\vec{1}_z M_{zz}\end{aligned} \tag{66}$$

which from (55) leads to (67), shown at the bottom of the page. Since the determinant will vanish if any diagonal entry is zero, (67) leads to

$$\begin{aligned}e^{-\Gamma}(1+\Gamma+\Gamma^2) &= \pm\frac{r^3 4\pi}{P_{xx}}\\ e^{-\Gamma}(1+\Gamma+\Gamma^2) &= \pm\frac{r^3 4\pi}{P_{yy}}\end{aligned} \tag{68}$$

which are essentially the same as (60) with a sign change and

$$e^{-\Gamma}(1-\Gamma) = \pm\frac{r^3 2\pi}{M_{zz}} \tag{69}$$

which is similar to (62) with a sign change and P_0 replaced with M_{zz}. The polarizability terms in (66) are related by $P_{xx} = P_{yy} = -2M_{zz}$ [17], with

$$M_{zz} = -\pi^2 b^3\left[\ln\left(\frac{8b}{a}\right)-2\right]^{-1}. \tag{70}$$

VII. Numerical Results

In order to demonstrate the accuracy of the presented formulation, the example of two identical thin perfectly conducting parallel wires separated by a distance $r = d$ is considered, as depicted in the insert of Fig. 3. The wires are in a mirror-symmetric configuration, which admits pure symmetric and antisymmetric modes. In all results to follow, both wires have $L/a = 200$ and the natural frequencies in the upper-half s-plane will be considered. For one such wire when isolated, the dominant resonance is at $(s^0_{1,1}L/C\pi) = -0.0865 + j0.9386$, computed from a rigorous electric field integral equation (IE) using a pulse basis and point matching [18]. Other resonances are available in the literature, e.g. [1], [20].

$$\det\begin{bmatrix} 1\pm\epsilon_0\frac{e^{-\gamma r}}{4\pi}P_{xx}(a_1+b_1) & 0 & 0 & 0 & \pm\epsilon_0\frac{e^{-\gamma r}}{4\pi}F_{e,m}2M_{zz} & 0\\ 0 & 1\pm\epsilon_0\frac{e^{-\gamma r}}{4\pi}P_{yy}(a_1+b_1) & 0 & \pm\epsilon_0\frac{e^{-\gamma r}}{4\pi}F_{e,m}2M_{zz} & 0 & 0\\ 0 & 0 & 1 & 0 & 0 & 0\\ 0 & 0 & 0 & 1 & 0 & 0\\ 0 & 0 & 0 & 0 & 1 & 0\\ 0 & 0 & 0 & 0 & 0 & 1\mp\epsilon_0\frac{e^{-\gamma r}}{4\pi}M_{zz}2a_1 \end{bmatrix} = 0 \tag{67}$$

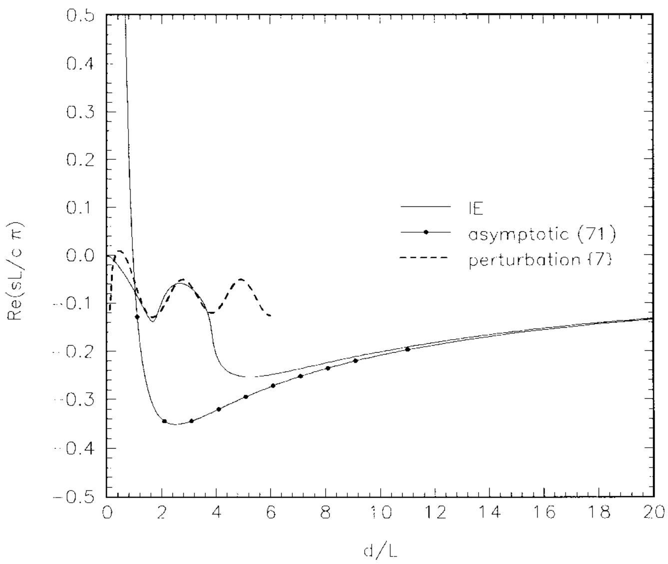

Fig. 6. Damping coefficient of lowest order antisymmetric mode of two identical parallel wires versus separation distance.

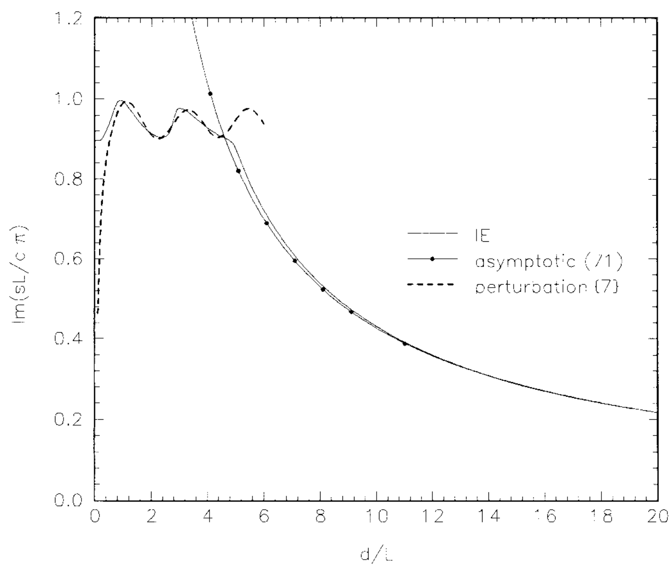

Fig. 7. Radian frequency of lowest order symmetric mode of two identical parallel wires versus separation distance.

For the coupled wire configuration described above, the asymptotic formulation (60) becomes s

$$e^{-\Gamma}(1+\Gamma+\Gamma^2) = \mp 103.1596\left(\frac{d}{L}\right)^3 \tag{71}$$

for $L/a = 200$. The migration of the lowest order antisymmetric and symmetric mode as a function of spacing d/L is shown in Figs. 3 and 4, respectively. The solution from an integral equation formulation [18], the perturbation method [6], and the asymptotic formulation (71) are shown. The solid box is the location of the isolated body resonance $s^0_{1,1}L/(c\pi)$. It can be seen that the spiraling behavior is essentially well described by the perturbation solution for intermediate spacings and the asymptotic solution agrees very well for larger spacings, as expected.

Figs. 5–8 show the radian frequency and damping coefficient for the lowest order antisymmetric and symmetric mode versus spacing d/L. For the modes considered in these figures, the asymptotic formulation (71) agrees very well with the exact (IE) solution for $d/L > 10$. Further results, and discussion of modal behavior and classification for many higher order modes are included in [19]. For all of the IE solutions presented, 20 pulses were used to generate the natural frequencies.

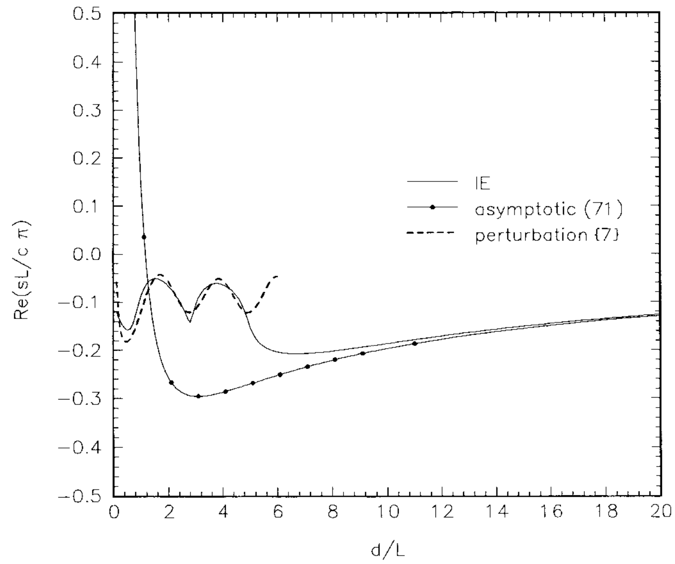

Fig. 8. Damping coefficient of lowest order symmetric mode of two identical parallel wires versus separation distance.

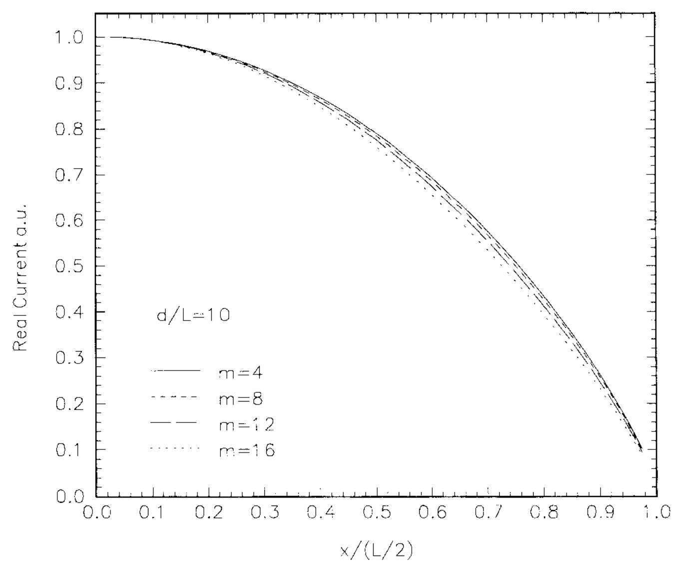

Fig. 9. Real part of symmetric natural mode current versus normalized wire length for the first four system modes at $d/L = 10$.

For the results in Figs. 3–8, (71) was solved numerically using a secant method root solver with initial guesses generated from an approximate solution of (71) [19]

$$\begin{aligned}\Gamma_m^{\binom{sy}{as}} &= \frac{s_m^{\binom{sy}{as}}}{C}\,d \\ &= \ln\left[0.023\,92 m^2\left(\frac{L}{d}\right)^3\right] + j\frac{m\pi}{2} \\ m &= \begin{pmatrix}4, 8, 12, \cdots \\ 2, 6, 10, \cdots\end{pmatrix}\end{aligned} \tag{72}$$

for $L/a = 200$.

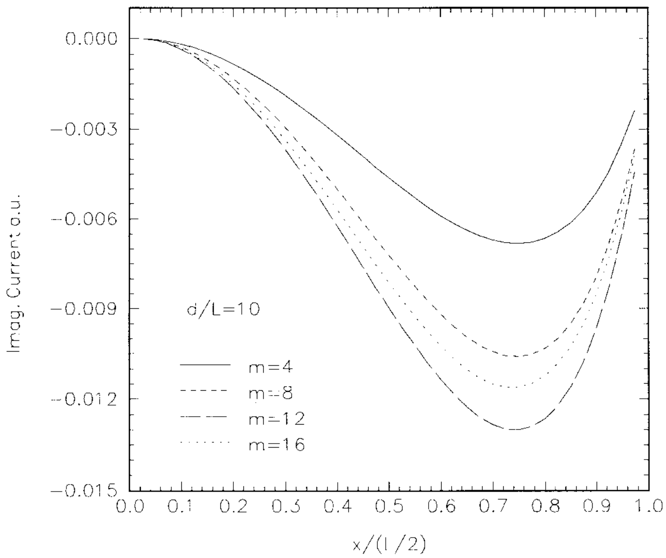

Fig. 10. Imaginary part of symmetric natural mode current versus normalized wire length for the first four system modes at $d/L = 10$.

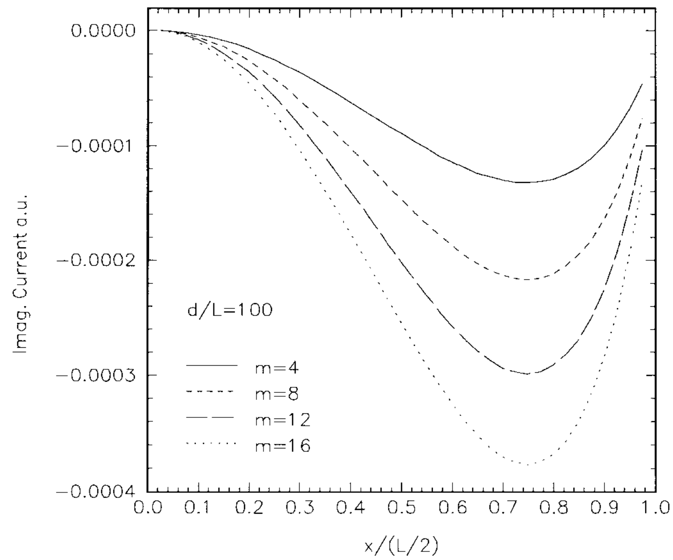

Fig. 12. Imaginary part of symmetric natural mode current versus normalized wire length for the first four system modes at $d/L = 100$.

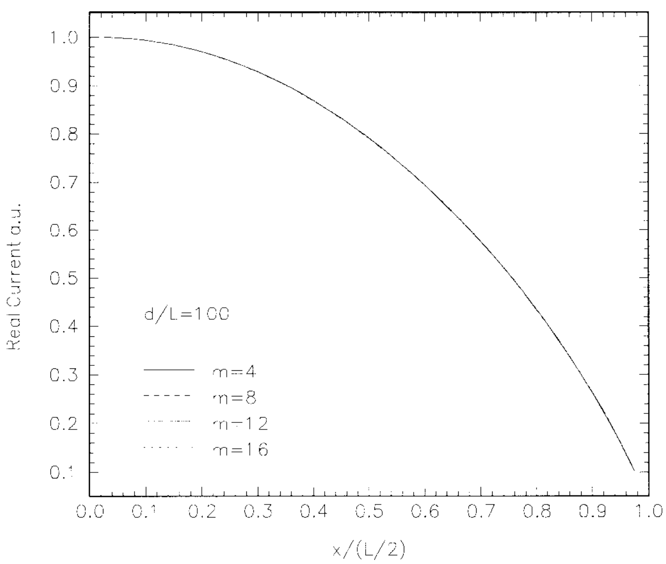

Fig. 11. Real part of symmetric natural mode current versus normalized wire length for the first four system modes at $d/L = 100$.

The natural mode current distribution of the first four symmetric modes $(m = 4, 8, 12, 16)$ are shown in Figs. 9 and 10 for $d/L = 10$ and in Figs. 11 and 12 for $d/L = 100$, obtained from an IE solution. It can be seen that all of the modes have associated dominant-like current distributions for large separations (which lead to low system frequencies), as would be expected. As $d/L \to \infty$, the current becomes nearly real and identical for each natural mode.

VIII. Conclusion

In this paper, we have examined the natural system frequencies of coupled bodies in the limit of large separation between all bodies. The general N-body problem is treated in the limit by replacing the bodies with equivalent dipole moments and solving the relevant scattering problem. Singular solutions of the scattering formulation lead to a transcendental equation, which may be solved to obtain the natural system frequencies of the coupled bodies. It has been found for two coupled wires that the real radian system frequency approaches the origin as $1/r$, independent of the relative orientation and type of the two bodies, and that the damping coefficient approaches the origin approximately logarithmically as a function of the body orientation and type. The asymptotic formulation is applied to the example of two parallel-coupled wires and a comparison between the asymptotic formulation and an integral equation solution is made, indicating the accuracy of the asymptotic formulation in the appropriate range.

Acknowledgment

The authors would like thank J. E. Ross for supplying the IE code.

References

[1] F. M. Tesche, "On the analysis of scattering and antenna problems using the singularity expansion technique," *IEEE Trans. Antennas Propagat.*, vol. AP-21, pp. 53–62, Jan. 1973.

[2] K. R. Umashankar, T. H. Shumpert, and D. R. Wilton, "Scattering by a thin wire parallel to a ground plane using the singularity expansion method," *IEEE Trans. Antennas Propagat.*, vol. AP-23, pp. 178–184, Mar. 1975.

[3] C. E. Baum, "Interaction of electromagnetic fields with an object which has an electromagnetic symmetry plane," Interaction Note 63, Mar., 1971.

[4] T. H. Shumpert and D. J. Galloway, "Finite length cylindrical scatterer near perfectly conducting ground. A transmission line mode approximation," *IEEE Trans. Antennas Propagat.*, vol. AP-26, pp. 145–151, Jan. 1978.

[5] L. S. Riggs and T. H. Shumpert, "Trajectories of the singularities of a thin wire scatterer parallel to a lossy ground," *IEEE Trans. Antennas Propagat.*, vol. AP-27, pp. 864–868, Nov. 1979.

[6] J. E. Ross, E. J. Rothwell, D. P. Nyquist, and K. M. Chen, "Approximate integral-operator methods for estimating the natural frequencies of coupled objects," *Radio Sci.*, vol. 29, pp. 677–684, 1994.

[7] C. E. Baum, T. H. Shumpert, and L. S. Riggs, "Perturbation of the SEM-pole parameters of an object by a mirror object," *Electromagn.*, vol. 8, pp. 169–186, 1989.

[8] G. W. Hanson and C. E. Baum, "Perturbation formula for the natural frequencies of an object in the presence of a layered medium," *Electromagn.*, vol. 18, no. 4, pp. 333–351, 1998.

[9] C. I. Chuang and D. P. Nyquist, "Perturbational formulation for nearly degenerate coupling," *1984 Nat. Radio Sci. Meet.*, Boulder, CO, Jan. 1984, p. 34.

[10] Y. Yuan and D. P. Nyquist, "Full-wave perturbation theory based upon electric field integral equation for coupled microstrip transmission lines," *IEEE Trans. Microwave Theory Tech.*, vol. 38, pp. 1576–1584, Nov. 1990.

[11] G. W. Hanson and D. P. Nyquist, "Full-wave perturbation theory for the analysis of coupled microstrip resonant structures," *IEEE Trans. Microwave Theory Tech.*, vol. 40, pp. 1774–1779, Sept. 1992.

[12] J. Van Bladel, *Singular Electromagnetic Fields and Sources*. New York: Oxford Univ. Press, 1991.

[13] A. D. Yaghjian, "Electric dyadic Green's functions in the source region," *Proc. IEEE*, vol. 68, pp. 248–263, Feb. 1980.

[14] C. E. Baum, "Some characteristics of electric and magnetic dipole antennas for radiating transient pulses," Sensor Simulation Note 125, Jan. 1971.

[15] C. E. Baum, T. K. Liu, and F. M. Tesche, "On the analysis of general multiconductor transmission-line networks," Interaction Note 350, Nov. 1978.

[16] K. S. H. Lee, "Electrically-small ellipsoidal antennas," Sensor Simulation Note 193, Feb. 1974.

[17] K. S. H. Lee, Ed., *EMP Interaction: Principles, Techniques, and Reference Data*. Philadelphia, PA: Taylor Francis, 1986.

[18] J. E. Ross, private communication.

[19] G. W. Hanson and C. E. Baum, "Asymptotic analysis of the natural system modes of coupled bodies in the large separation, low-frequency regime," Interaction Note 528, July 1997.

[20] F. M. Tesche, "On the singularity expansion method as applied to electromagnetic scattering from thin-wires," Interaction Note 102, Apr. 1972.

[21] C. E. Baum and H. N. Kritikos, Eds., *Electromagnetic Symmetry*. Washington, DC: Taylor Francis, 1995.

[22] C. E. Baum, T. H. Shumpert, and L. S. Riggs, "Perturbation of the SEM-pole parameters of an object by a mirror object," Sensor Simulation Note 309, Sept. 1987.

George W. Hanson (S'85–M'91) was born in Glen Ridge, NJ, in 1963. He received the B.S.E.E. degree from Lehigh University, Bethlehem, PA, the M.S.E.E. degree from Southern Methodist University, Dallas, TX, and the Ph.D. degree from Michigan State University, East Lansing, in 1986, 1988, and 1991, respectively.

From 1986 to 1988, he was a Development Engineer with General Dynamics, Fort Worth, TX, where he worked on radar simulators. From 1988 to 1991 he was a Research and Teaching Assistant in the Department of Electrical Engineering, Michigan State University. He is currently an Associate Professor of electrical engineering and computer science at the University of Wisconsin, Milwaukee. His research interests include electromagnetic wave phenomena in layered media and microwave characterization of materials.

Dr. Hanson is a member of URSI Commission B, Sigma Xi and Eta Kappa Nu.

Carl E. Baum (S'62–M'63–SM'78–F'84) was born in Binghamton, NY, on February 6, 1940. He received the B.S. (honors), M.S., and Ph.D. degrees in electrical engineering from the California Institute of Technology, Pasadena, in 1962, 1963, and 1969, respectively.

In 1962, he was commissioned in the United States Air Force and was stationed at the Air Force Research Laboratory, Directed Energy Directorate (formerly Phillips Laboratory, formerly Air Force Weapons Laboratory) from 1963 to 1967 and from 1968 to 1971. Since 1971 he has served as a civil servant with a position as Senior Scientist at the Air Force Research Laboratory. He is an advisor to numerous government agencies on high-power electromagnetics (HPE) related matters and represents the U.S. in exchanging such information with various countries. He is editor of several interagency note series on EMP and related subjects and has been a Distinguished Lecturer of the IEEE Antennas and Propagation Society. He has published three books: *Transient Lens Synthesis: Differential Geometry in Electromagnetic Theory*, (Philadelphia, PA: Taylor and Francis, 1995 [coauthor A. P. Stone]), *Electromagnetic Symmetry* (Philadelphia, PA: Taylor and Francis, 1997 [coeditor H. N. Kritikos]), and *Ultra-Wideband, Short Pulse Electromagnetics 3* (New York: Plenum). He has written many book chapters and his papers have won various awards. He has led an EMP short course and HPE workshop at numerous locations around the globe.

Dr. Baum has received the Richard R. Stoddart Award of the IEEE EMC Society (October 1984) with the citation: "for service as the scientific organizer and editor of EMP technical publications." He has been named by the IEEE Board of Directors recipient of the 1987 Harry Diamond Memorial Award with citation: "for outstanding contributions to the knowledge of transient phenomena in electromagnetics." He is cochairman (for the IEEE Antennas and Propagation Society) of the Joint Technical Committee on High-Power Electromagnetics. is a member of Tau Beta Pi and Sigma Xi. He is a member of Commissions A, B, and E of the U.S. National Committee of the International Union of Radio Science (URSI), is a past chairman of the International Commission E Working Group: "Scientific Basis for Noise and Interface Control," and cochairman of the working group: "Interaction with and Protection of Complex Electrical Systems," and has been a U.S. delegate to numerous URSI General Assemblies around the world. and won the Honeywell Award as best undergraduate engineer in 1962. His numerous contributions to transient electrmagnetics technology and electromagnetic theory have resulted in election to fellow the IEEE (January 1, 1984) with citation: "for pioneering the singularity expansion method and electromagnetic topology in electromagnetic theory, and for the development of EMP simulation and electromagnetic sensors." He is a member of the Electromagntics Academy and the New Mexico Academy of Science and is past president of the Electromagnetics Society. He is an EMP Fellow and founder and president of SUMMA Foundation, which sponsors various electromagnetics related activities includng scientific conferences, publications, short courses, fellowships, and awards. He was awarded the Air Force Research and Development Award (1970), the AFSC Harold Brown Award (1990), and Phillips Laboratory Fellow (1996).